

# Bifurcation Analysis of an Anaerobic Digestion System

Mihaela Sbarciog  
Automatic Control Laboratory  
University of Mons  
31 Boulevard Dolez  
7000 Mons, Belgium  
MihaelaIuliana.Sbarciog@UMons.ac.be

Alain Vande Wouwer  
Automatic Control Laboratory  
University of Mons  
31 Boulevard Dolez  
7000 Mons, Belgium  
Alain.VandeWouwer@UMons.ac.be

**Abstract**—This paper presents the bifurcation analysis of an anaerobic digestion model, which includes hydrogen production along with methane production. Analytical expressions of the equilibria are given and the conditions for their occurrence are provided. The analytical developments are validated by means of bifurcation diagrams built with specialized continuation software. Special emphasis is put on revealing the relationship between hydrogen and methane outflow rate. The complex system behavior is illustrated by means of phase portraits.

**Index Terms**—nonlinear systems, bifurcation analysis, anaerobic digestion

## I. INTRODUCTION

Anaerobic digestion denotes a series of biological transformations in which organic matter is degraded by several microbial populations in the absence of oxygen. During the process, biogas is produced, which can be used for electricity and heat generation, or can be processed into renewable natural gas and transportation fuels. Anaerobic digestion has become the preferred waste treatment method, due to its ability to process high organic loads and to generate less sludge to be disposed. However, due to the process complexity which makes it difficult to understand and operate, anaerobic digestion is not yet used at its full potential.

One of the main difficulties in understanding and controlling the anaerobic digestion process comes from the lack of measurements, which hampers the comprehension of the relationships between the various variables of the system. In an attempt to alleviate this issue and to provide a platform for research and developments in anaerobic digestion, a general model has been proposed, ie. the anaerobic digestion model no.1 (ADM1) [1], which models all the stages appearing in the process. As a consequence, a high dimensional model has been obtained, consisting of 35 differential equations coupled with 8 algebraic equations, which has been continuously adapted and extended to accommodate various types of waste. The ADM1 model is too complex to be used for control design purposes, where generally one-, two- or three-step models are employed. However, it has been successfully used as a system emulator for developing reduced order models [2] or testing control and observation algorithms [3]. A steady state analysis

of ADM1 has been performed in [4] employing continuation software, with the aim of emphasizing the mechanisms which should be taken in a reduced order model in order to capture the main process dynamics, as many two-step models that have been used extensively for control design do not show the same behavior as ADM1.

The bifurcation analysis of anaerobic digestion models has been considered by many researchers (eg. [5], [6]), as the system complexity is reflected by its steady state multiplicity. The steady state analysis allows to detect the conditions which trigger the anaerobic digestion instability, that is generally assessed as the lost ability of the system to produce biogas. The biogas produced through anaerobic digestion is a mix of methane, hydrogen and carbon dioxide. Often the emphasis is on producing methane, and the control criteria are formulated such as to maximize the outflow rate of methane. However, hydrogen production by the anaerobic digestion of organic substrates becomes more and more popular, and the question that arises is whether or not the same system could be used alternatively for methane production and hydrogen production. Even when the goal is to maximize the methane production, there are experimental studies which indicate that the hydrogen concentration is a fast and reliable indicator for process stability. Therefore, revealing the relationships between methane and hydrogen could bring valuable insight into process dynamics and would allow the development of control strategies that could be easier implemented in practice, as gas measurements are widely available on biogas plants.

In this paper, a model of the anaerobic digestion process is considered, which characterizes also the evolution of the hydrogen concentration inside the reactor along with the methane production. A slightly modified version of this model has been considered in [7], where the steady state behavior of the system has been studied numerically. Here, we provide analytical expressions for the system equilibria, analytical conditions for the occurrence of the equilibria and we discuss the steady state relationship between hydrogen concentration and methane outflow rate. Bifurcation diagrams obtained numerically and simulated phase portraits of the system are included as a validation for the analytical results. A comparison of the obtained results with the steady state

analysis of the ADM1 model [4] indicate that the model considered here exhibits the same complexity of the steady state behavior as ADM1.

## II. MODEL DESCRIPTION

The model studied throughout this paper includes three stages of the anaerobic digestion process [7], acidogenesis, acetogenesis and methanogenesis, and involves four nutrient groups and the corresponding bacterial groups: simple substrates  $S$ , volatile fatty acids  $V$ , acetic acid  $A$ , hydrogen  $H$ , acidogenic bacteria  $X_S$ , acetogenic bacteria  $X_V$ , acetoclastic methanogens  $X_A$  and hydrogenotrophic methanogens  $X_H$ . The model has the general structure

$$\dot{\xi} = D(\xi_{in} - \xi) - F + Kr(\xi) \quad (1)$$

where  $D$  is the dilution rate representing the influent flow scaled by the reactor volume,  $\xi$  is the state vector made of concentrations of components in the reactor,  $\xi_{in}$  is the vector of inlet concentrations,  $F$  is the rate of removal in gaseous form of components,  $K$  is the matrix of stoichiometric coefficients and  $r(\xi)$  represents the vector of reaction rates.

Neglecting the transfer from liquid to the gas phase the mass balances for each component read:

$$\frac{dX_S}{dt} = -DX_S + g_S(S)X_S \quad (2)$$

$$\frac{dX_V}{dt} = -DX_V + g_V(V, H)X_V \quad (3)$$

$$\frac{dX_A}{dt} = -DX_A + g_A(A)X_A \quad (4)$$

$$\frac{dX_H}{dt} = -DX_H + g_H(H, A)X_H \quad (5)$$

$$\frac{dS}{dt} = D(S_{in} - S) - k_1g_S(S)X_S \quad (6)$$

$$\frac{dV}{dt} = -DV + k_2g_S(S)X_S - k_3g_V(V, H)X_V \quad (7)$$

$$\frac{dA}{dt} = -DA + k_4g_S(S)X_S + k_5g_V(V, H)X_V - k_6g_A(A)X_A \quad (8)$$

$$\frac{dH}{dt} = -DH + k_7g_S(S)X_S + k_8g_V(V, H)X_V - k_9g_H(H, A)X_H \quad (9)$$

while the rate of methane production is given by:

$$Q_M = k_{10}g_A(A)X_A + k_{11}g_H(H, A)X_H \quad (10)$$

In (2)- (10),  $S_{in}$  is the concentration of nutrient in the influent flow,  $k_i$ ,  $i = 1 \dots 11$  are the stoichiometric parameters, while  $g_j$ ,  $j \in \{S, V, A, H\}$  denote the growth functions. The growth functions depend on the concentration of the component that is decomposed and other factors that might inhibit the reaction. Further on, we use the explicit forms of the growth functions:

$$g_S(S) = \frac{m_S S}{K_S + S}, g_V(V, H) = \frac{m_V V}{K_V + V + \mu_H H}$$

$$g_A(A) = \frac{m_A A}{K_A + A + A^2/K_I}, g_H(H, A) = \frac{m_H H}{K_H + H + \mu_A A}$$

TABLE I  
NUMERICAL VALUES OF THE PARAMETERS

Parameter	Value	Parameter	Value
$m_S$	$3.5\text{day}^{-1}$	$K_S$	0.4g COD/L
$m_V$	$0.86\text{day}^{-1}$	$K_V$	0.3g COD/L
$m_A$	$0.4\text{day}^{-1}$	$K_A$	0.15g COD/L
$m_H$	$2.1\text{day}^{-1}$	$K_H$	2.5e-5g COD/L
$S_{in}$	40g COD/L	$\mu_H$	1
$K_I$	10g COD/L	$\mu_A$	5

where  $m_j$  and  $K_j$ , with  $j \in \{S, V, A, H\}$  respectively denote the maximum growth rates and the half-saturation constants in the absence of inhibition;  $K_I$  is a coefficient describing the inhibition due to  $A$  on the growth of  $X_A$ ;  $\mu_H$  and  $\mu_A$  are inhibition factors for the growth of  $X_V$  and  $X_H$  respectively due to  $H$  and  $A$ . The numerical values of the kinetic parameters are given in Table I, while the stoichiometric parameters are:  $k_1 = 11.11$ ,  $k_2 = 1.962$ ,  $k_3 = 20$ ,  $k_4 = 6.419$ ,  $k_5 = 10.357$ ,  $k_6 = 20$ ,  $k_7 = 2.367$ ,  $k_8 = 5.268$ ,  $k_9 = 16.667$ ,  $k_{10} = 19$ ,  $k_{11} = 15.667$ .

As proved in [7], all solutions of (2)- (9) with nonnegative initial conditions remain nonnegative and are bounded. Further on, we make use explicitly of the mathematical expressions of the system growth functions to analytically compute and characterize the equilibria. This is particularly important in view of efficiently operating and controlling the anaerobic digestion process.

## III. CALCULATION AND CHARACTERIZATION OF THE STEADY STATES

To simplify the computation and characterization of the system equilibria, we use a well-known canonical state transformation, which reduces the system dynamics to the so called reaction manifold [8]. Let us consider the state transformation  $\xi = [\xi_a \ \xi_b]'$   $\mapsto$   $x = [x_a \ x_b]'$ , with  $x_a = \xi_a = [X_S \ X_V \ X_A \ X_H]'$  and  $x_b$  given by

$$x_b = \begin{bmatrix} S + k_1 X_S \\ V - k_2 X_S + k_3 X_V \\ A - k_4 X_S - k_5 X_V + k_6 X_A \\ H - k_7 X_S - k_8 X_V + k_9 X_H \end{bmatrix} \quad (11)$$

The state equations are rewritten as:

$$\dot{x}_1 = \frac{dX_S}{dt} = -Dx_1 + g_S(S)x_1 \quad (12)$$

$$\dot{x}_2 = \frac{dX_V}{dt} = -Dx_2 + g_V(V, H)x_2 \quad (13)$$

$$\dot{x}_3 = \frac{dX_A}{dt} = -Dx_3 + g_A(A)x_3 \quad (14)$$

$$\dot{x}_4 = \frac{dX_H}{dt} = -Dx_4 + g_H(H, A)x_4 \quad (15)$$

$$\dot{x}_5 = D(S_{in} - x_5) \quad (16)$$

$$\dot{x}_6 = -Dx_6 \quad (17)$$

$$\dot{x}_7 = -Dx_7 \quad (18)$$

$$\dot{x}_8 = -Dx_8 \quad (19)$$

The system dynamics converges to the space

$$S_x = \{x \in \mathbb{R}^8 \mid x_5 = S_{in}, x_6 = 0, x_7 = 0, x_8 = 0\}$$

All system equilibria lie in  $S_x$ , which implies that at equilibrium:

$$S + k_1 X_S = S_{in} \quad (20)$$

$$V - k_2 X_S + k_3 X_V = 0 \quad (21)$$

$$A - k_4 X_S - k_5 X_V + k_6 X_A = 0 \quad (22)$$

$$H - k_7 X_S - k_8 X_V + k_9 X_H = 0 \quad (23)$$

The system steady states are the solutions of

$$(-D + g_S(S)) \cdot x_1 = 0 \quad (24)$$

$$(-D + g_V(V, H)) \cdot x_2 = 0 \quad (25)$$

$$(-D + g_A(A)) \cdot x_3 = 0 \quad (26)$$

$$(-D + g_H(H, A)) \cdot x_4 = 0 \quad (27)$$

which lead to several possibilities detailed below. Note that from a practical point of view, we are interested in the physical steady states, characterized by nonnegative values of all state components. Therefore the conditions for physical steady states are derived by requiring that  $\bar{\xi}_i > 0$  for  $i = 1, 8$ , i.e. the value of the state at equilibrium. These conditions and the analytical expressions of the equilibria are summarized in Table II and detailed elsewhere.

- 1)  $x_1 = 0$  ( $X_S = 0$ ): In this case, the only physical equilibrium of the system is the total wash-out state, where no conversion takes place. This steady state occurs independent of the dilution rate and the concentration of substrate in the influent. In physical states, the total wash-out steady state is given by:

$$\xi^W = [0 \ 0 \ 0 \ 0 \ S_{in} \ 0 \ 0 \ 0]'$$

- 2)  $g_S(S) = D$ ,  $x_2 = x_3 = x_4 = 0$  ( $X_V = X_A = X_H = 0$ ): This steady state is characterized by the degradation of the organic substrate and the wash-out of the acetogenic bacteria, acetoclastic methanogens and hydrogenotrophic methanogens. Since no methanogenic biomass is present in the reactor, there will be no methane production. The equilibrium point

$$\xi^0 = [\bar{X}_S \ 0 \ 0 \ 0 \ \bar{S} \ \bar{V} \ \bar{A} \ \bar{H}]'$$

is a conditional physical equilibrium point.

- 3)  $g_S(S) = D$ ,  $g_V(V, H) = D$ ,  $x_3 = x_4 = 0$  ( $X_A = X_H = 0$ ): The corresponding steady state

$$\xi^V = [\bar{X}_S \ \bar{X}_V \ 0 \ 0 \ \bar{S} \ \bar{V} \ \bar{A} \ \bar{H}]'$$

is characterized by the conversion of the substrate into VFAs which are further processed to acetic acid. Since none of the methanogens are present in the reactor, no methane production occurs. This equilibrium point is physical if the conditions stated in Table II are fulfilled.

- 4)  $g_S(S) = D$ ,  $g_V(V, H) = D$ ,  $g_A(A) = D$ ,  $x_4 = 0$  ( $X_H = 0$ ): The equation  $g_A(A) = D$  has two real solutions  $\bar{A}_i$ ,  $i = 1, 2$ , with  $\bar{A}_1 < \bar{A}_2$  if

$$D < \max(g_A(A)) = g_A(\sqrt{K_A K_I}) \quad (28)$$

Rewriting  $g_A(A) = D$  as

$$A^2 + K_I \frac{(D - m_A)}{D} + K_A K_I = 0 \quad (29)$$

one may find the solutions  $\bar{A}_i$ ,  $i = 1, 2$ . There may be up to two equilibria of this type

$$\xi_i^{VA} = [\bar{X}_S \ \bar{X}_V \ \bar{X}_{A_i} \ 0 \ \bar{S} \ \bar{V} \ \bar{A}_i \ \bar{H}]'$$

The steady states  $\xi_i^{VA}$  are characterized by methane production.

- 5)  $g_S(S) = D$ ,  $x_2 = x_3 = 0$  ( $X_V = X_A = 0$ ),  $g_H(H, A) = D$ : One equilibrium occurs in this situation,

$$\xi^H = [\bar{X}_S \ 0 \ 0 \ \bar{X}_H \ \bar{S} \ \bar{V} \ \bar{A} \ \bar{H}]'$$

which is a physical steady state if all the states are nonnegative. The steady state  $\xi^H$  is characterized by the wash-out of the acetogenic bacteria  $\bar{X}_V$  and acetoclastic methanogens  $\bar{X}_A$  but some methane production is ensured by the presence of the hydrogenotrophic methanogens  $\bar{X}_H$ .

- 6)  $g_S(S) = D$ ,  $g_V(V, H) = D$ ,  $X_A = 0$ ,  $g_H(H, A) = D$ : This possibility leads to the equilibrium point

$$\xi^{VH} = [\bar{X}_S \ \bar{X}_V \ 0 \ \bar{X}_H \ \bar{S} \ \bar{V} \ \bar{A} \ \bar{H}]'$$

where again the methane generation is ensured by the presence of hydrogenotrophic methanogens  $\bar{X}_H$ .

- 7)  $g_S(S) = D$ ,  $X_V = 0$ ,  $g_A(A) = D$ ,  $g_H(H, A) = D$ : Up to two equilibria

$$\xi_i^{AH} = [\bar{X}_S \ 0 \ \bar{X}_{A_i} \ \bar{X}_{H_i} \ \bar{S} \ \bar{V} \ \bar{A}_i \ \bar{H}_i]'$$

may be obtained. Both of them are characterized by methane production which occurs through both methanogenic pathways.

- 8)  $g_S(S) = D$ ,  $X_V = 0$ ,  $g_A(A) = D$ ,  $X_H = 0$ : In this case also at most two equilibrium points may be obtained. These equilibria have the form

$$\xi_i^A = [\bar{X}_S \ 0 \ \bar{X}_{A_i} \ 0 \ \bar{S} \ \bar{V} \ \bar{A}_i \ \bar{H}]'$$

The methane production is ensured by the presence of the hydrogenotrophic methanogens.

- 9)  $g_S(S) = D$ ,  $g_V(V, H) = D$ ,  $g_A(A) = D$ ,  $g_H(H, A) = D$ : This alternative also leads to up to two equilibria

$$\xi_i^* = [\bar{X}_S \ \bar{X}_{V_i} \ \bar{X}_{A_i} \ \bar{X}_{H_i} \ \bar{S} \ \bar{V}_i \ \bar{A}_i \ \bar{H}_i]'$$

which are characterized by the coexistence of all species. Consequently, methane is produced through both methanogenic pathways.

#### IV. BIFURCATION DIAGRAMS AND SYSTEM PHASE PORTRAIT

The analytical computation of equilibria presented in Section III allows us to determine not only the type of equilibria in which the anaerobic digestion system produces methane (hydrogen is produced in all steady states except of the total wash-out condition), but also to classify these equilibria in terms

TABLE II  
ANALYTICAL EXPRESSIONS AND CONDITIONS FOR OCCURRENCE OF THE EQUILIBRIA

Equilibrium	Expression	Conditions
$\xi^W$	$\bar{X}_S = 0, \bar{X}_V = 0, \bar{X}_A = 0, \bar{X}_H = 0$ $\bar{S} = S_{in}, \bar{V} = 0, \bar{A} = 0, \bar{H} = 0$	-
$\xi^0$	$\bar{X}_S = \frac{(S_{in}-\bar{S})}{k_1}, \bar{X}_V = 0, \bar{X}_A = 0, \bar{X}_H = 0$ $\bar{S} = DK_S/(m_S - D), \bar{V} = k_2/k_1(S_{in} - \bar{S})$ $\bar{A} = k_4/k_1(S_{in} - \bar{S}), \bar{H} = k_7/k_1(S_{in} - \bar{S})$	$D < m_S$ $\bar{S} < S_{in}$
$\xi^V$	$\bar{X}_S = \frac{(S_{in}-\bar{S})}{k_1}, \bar{X}_V = \frac{k_2\bar{X}_S - \bar{V}}{k_3}, \bar{X}_A = 0, \bar{X}_H = 0$ $\bar{S} = \frac{DK_S}{(m_S - D)}, \bar{V} = \frac{D(K_V + \mu_H\bar{H})}{(m_V - D)}, \bar{A} = k_4\bar{X}_S + k_5\bar{X}_V$ $\bar{H} = \left( \frac{(k_3k_7 + k_8k_2)}{k_3} \bar{X}_S - \frac{k_8}{k_3} \frac{DK_V}{(m_V - D)} \right) / \left( 1 + \frac{k_8}{k_3} \frac{D\mu_H}{(m_V - D)} \right)$	$D < m_S, \bar{S} < S_{in}$ $D < m_V, \frac{k_1}{k_2}\bar{V} + \bar{S} < S_{in}$
$\xi_i^{VA}$	$\bar{X}_S = \frac{(S_{in}-\bar{S})}{k_1}, \bar{X}_V = \frac{k_2\bar{X}_S - \bar{V}}{k_3}$ $\bar{X}_{A_i} = \frac{1}{k_6}(k_4\bar{X}_S + k_5\bar{X}_V - \bar{A}_i), \bar{X}_H = 0$ $\bar{S} = \frac{DK_S}{(m_S - D)}, \bar{V} = \frac{D(K_V + \mu_H\bar{H})}{(m_V - D)}, \bar{A}_i$ from (29) $\bar{H} = \left( \frac{(k_3k_7 + k_8k_2)}{k_3} \bar{X}_S - \frac{k_8}{k_3} \frac{DK_V}{(m_V - D)} \right) / \left( 1 + \frac{k_8}{k_3} \frac{D\mu_H}{(m_V - D)} \right)$	$D < m_S, \bar{S} < S_{in}, D < m_V$ $D < \max(g_A(A)), \frac{k_1}{k_2}\bar{V} + \bar{S} < S_{in}$ $k_3c_1\bar{A}_i + k_5c_1\bar{V} + \bar{S} < S_{in}$
$\xi^H$	$\bar{X}_S = \frac{(S_{in}-\bar{S})}{k_1}, \bar{X}_V = 0, \bar{X}_A = 0, \bar{X}_H = \frac{1}{k_9}(k_7\bar{X}_S - \bar{H})$ $\bar{S} = \frac{DK_S}{(m_S - D)}, \bar{V} = k_2\bar{X}_S, \bar{A} = k_4\bar{X}_S, \bar{H} = \frac{D(K_H + \mu_A k_4\bar{X}_S)}{(m_H - D)}$	$D < m_S, \bar{S} < S_{in}, D < m_H$ $\frac{k_1}{k_7}\bar{H} + \bar{S} < S_{in}$
$\xi^{VH}$	$\bar{X}_S = \frac{(S_{in}-\bar{S})}{k_1}, \bar{X}_V = \frac{k_2\bar{X}_S - \bar{V}}{k_3}$ $\bar{X}_A = 0, \bar{X}_H = \frac{1}{k_9}(k_7\bar{X}_S + k_8\bar{X}_V - \bar{H})$ $\bar{S} = \frac{DK_S}{(m_S - D)}, \bar{A} = k_4\bar{X}_S + k_5\bar{X}_V, \bar{H} = \frac{D(K_H + \mu_A\bar{A})}{(m_H - D)}$ $\bar{V} = \frac{D(K_V(m_H - D) + \mu_H D(K_H + \mu_A\bar{X}_S \frac{(k_3k_4 + k_5k_2))}{k_3}))}{((m_V - D)(m_H - D) + \mu_H\mu_A D^2 \frac{k_5}{k_3})}$	$D < m_S, \bar{S} < S_{in}$ $D < m_V, D < m_H$ $\frac{k_1}{k_2}\bar{V} + \bar{S} < S_{in}$ $k_3c_2\bar{H} + k_8c_2\bar{V} + \bar{S} < S_{in}$
$\xi_i^{AH}$	$\bar{X}_S = \frac{(S_{in}-\bar{S})}{k_1}, \bar{X}_V = 0$ $\bar{X}_{A_i} = \frac{1}{k_6}(k_4\bar{X}_S - \bar{A}_i), \bar{X}_H = \frac{1}{k_9}(k_7\bar{X}_S - \bar{H}_i)$ $\bar{S} = \frac{DK_S}{(m_S - D)}, \bar{V} = k_2\bar{X}_S, \bar{A}_i$ from (29), $\bar{H}_i = D \frac{(K_H + \mu_A\bar{A}_i)}{(m_H - D)}$	$D < m_S, \bar{S} < S_{in}, D < \max(g_A(A))$ $D < m_H, \frac{k_1}{k_4}\bar{A}_i + \bar{S} < S_{in}$ $\frac{k_1}{k_7}\bar{H}_i + \bar{S} < S_{in}$
$\xi_i^A$	$\bar{X}_S = \frac{(S_{in}-\bar{S})}{k_1}, \bar{X}_V = 0, \bar{X}_{A_i} = \frac{1}{k_6}(k_4\bar{X}_S - \bar{A}_i), \bar{X}_H = 0$ $\bar{S} = \frac{DK_S}{(m_S - D)}, \bar{V} = k_2\bar{X}_S, \bar{A}_i$ from (29), $\bar{H} = k_7\bar{X}_S$	$D < m_S, \bar{S} < S_{in}, D < \max(g_A(A))$ $\frac{k_1}{k_4}\bar{A}_i + \bar{S} < S_{in}$
$\xi_i^*$	$\bar{X}_S = \frac{(S_{in}-\bar{S})}{k_1}, \bar{X}_{V_i} = \frac{1}{k_3}(k_2\bar{X}_S - \bar{V}_i)$ $\bar{X}_{A_i} = \frac{1}{k_6}(k_4\bar{X}_S + k_5\bar{X}_{V_i} - \bar{A}_i),$ $\bar{X}_{H_i} = \frac{1}{k_9}(k_7\bar{X}_S + k_8\bar{X}_{V_i} - \bar{H}_i), \bar{S} = \frac{DK_S}{(m_S - D)}$ $\bar{V}_i = D \frac{(K_V + \mu_H\bar{H}_i)}{(m_V - D)}, \bar{A}_i$ from (29), $\bar{H}_i = D \frac{(K_H + \mu_A\bar{A}_i)}{(m_H - D)}$	$D < m_S, \bar{S} < S_{in}, D < \max(g_A(A))$ $D < m_V, D < m_H, \frac{k_1}{k_2}\bar{V}_i + \bar{S} < S_{in}$ $k_3c_1\bar{A}_i + k_5c_1\bar{V}_i + \bar{S} < S_{in}$ $k_3c_2\bar{H}_i + k_8c_2\bar{V}_i + \bar{S} < S_{in}$

of their methane productivity. However, since the anaerobic digestion process is operated by means of the dilution rate, it would be interesting to have a view on the change in the methane outflow rate and in the concentration of hydrogen as the dilution rate is changed. Such a graphical representation is the one-parameter bifurcation diagram (i.e. the dilution rate is varied while the inlet substrate concentration is kept constant). In principle such a bifurcation diagram may be constructed for each of the system states. Here we present only the diagrams for methane outflow rate and hydrogen concentration.

The one-parameter bifurcation diagrams can be constructed by using the expression of equilibria given in Table II for various dilution rate values. Alternatively, one may use a continuation software, which computes the bifurcation diagrams numerically without requiring any prior knowledge on the system dynamics. The diagrams presented in Figs. 1 and 2 are obtained by employing such a software, namely MatCONT [9], as a way of verifying the correctness of the calculations presented in Section III.

Figs. 1 and 2 illustrate all equilibrium branches detailed in

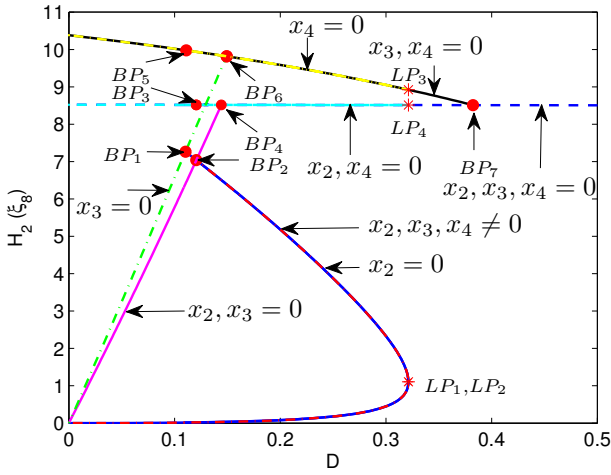


Fig. 1. Bifurcation diagram for the hydrogen concentration

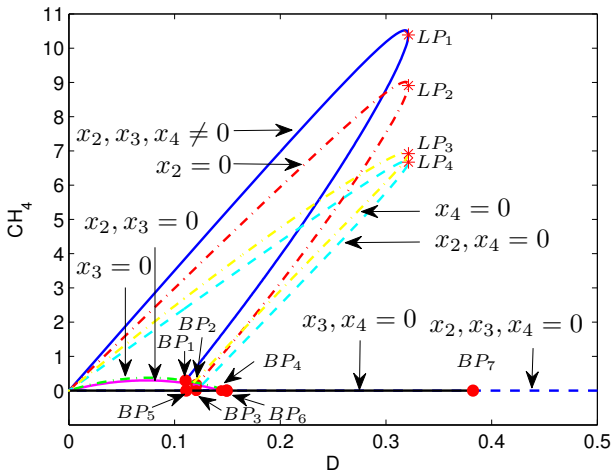


Fig. 2. Bifurcation diagram for the methane outflow rate

Section III, except from the trivial solution, the total wash-out solution. Each branch is presented in a different color and type of line and a label has been assigned to it, which indicates the mechanism that leads to the occurrence of the equilibria and allows their identification. For example, the label  $x_2, x_3, x_4 \neq 0$  indicates that the equilibrium occurs when all types of biomass are present in the reactor (this corresponds to choice 9 in the list), thus the branch corresponds to the equilibria  $\xi_i^*$ . Characteristic for one-parameter bifurcation diagrams are the limit points (denoted by  $LP$ ) and branch points (denoted by  $BP$ ). The limit points indicate that the specific equilibrium ceases to exist for dilution rates higher than the one corresponding to the limit point. The branch points indicate that two distinct equilibrium branches come together, of which one ceases to exist. There are four limit points and seven branch points, respectively shown in Figs. 1 and 2 with a star and a bullet. Since the limit points and the branch points indicate the occurrence/disappearance of the equilibria, their coordinates can be computed from the conditions for physical equilibria listed in Table II.

The number of equilibrium points which occur for a certain

dilution rate is given by the number of branches encountered at that specific dilution rate. Note that in Fig. 1, there are two branches of type  $x_2, x_4 = 0$  for dilution rates between the values corresponding to  $BP_3$  and  $LP_4$ , and two branches of type  $x_4 = 0$  for dilution rates between the values corresponding to  $BP_5$  and  $LP_3$ . This becomes evident in Fig. 2. For example, at the dilution rate  $D = 0.3$ , the system has 11 equilibrium points: two for  $x_2, x_3, x_4 \neq 0$  ( $\xi_1^*$  and  $\xi_2^*$ ), two for  $x_2 = 0$  ( $\xi_1^{AH}$  and  $\xi_2^{AH}$ ), two for  $x_2, x_4 = 0$  ( $\xi_1^A$  and  $\xi_2^A$ ), two for  $x_4 = 0$  ( $\xi_1^{VA}$  and  $\xi_2^{VA}$ ), one for  $x_3, x_4 = 0$  ( $\xi^V$ ), one for  $x_2, x_3, x_4 = 0$  ( $\xi^0$ ) and the total wash-out ( $\xi^W$ ), which is not indicated on the bifurcation diagrams.

Since hydrogen is consumed by the hydrogenotrophic methanogens  $x_4$  to produce methane, it is obvious that hydrogen and methane production cannot be maximum at the same time. In fact, the highest hydrogen concentration is achieved when the hydrogenotrophic methanogens have been washed-out ( $x_4 = 0$ ), which in turn corresponds to either a lower methane production if the acetoclastic methanogens are still present in the reactor (branch  $x_4 = 0$ ) or zero methane production if the acetoclastic methanogens have been also washed-out (branch  $x_3, x_4 = 0$ ). Qualitatively similar results are described by the branch  $x_2, x_4 = 0$ , which indicates that the presence of the acetogenic bacteria  $x_2$  in the previous case ( $x_4 = 0$ ) generates an increase in the hydrogen concentration, which diminishes however when the dilution rate increases. This increase is also observed in the methane outflow rate. On the contrary, the highest methane production is achieved when all types of biomass are present in the reactor (branch  $x_2, x_3, x_4 \neq 0$ ). Compared to the branch  $x_2 = 0$ , higher methane outflow rate is obtained but the same concentration of hydrogen is achieved.

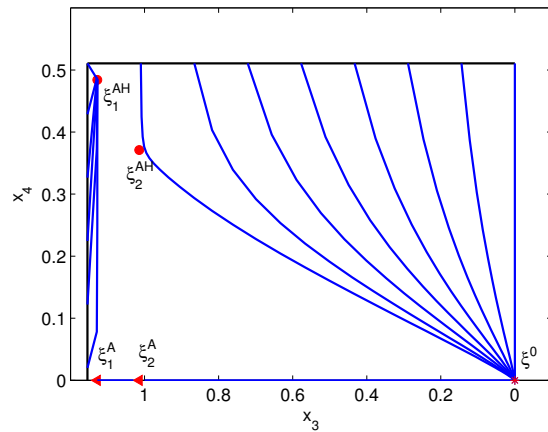


Fig. 3. The system phase portrait on the invariant set  $x_2 = 0$

In the following, the system steady state multiplicity is illustrated by means of the system phase portrait for the dilution rate  $D = 0.3$ . Taking into account the high dimensionality of the system, and the fact that the system dynamics converge to the space  $S_x$  which contains all system equilibria, without loss of generality the phase portrait is restricted to the space  $S_x$ . Furthermore, note that except for the total system wash-

out, all steady states lie on the hyperplane  $x_2 = \bar{X}_S$ . Hence a three dimensional representation of the phase portrait on the hyperspace  $S_x \cap x_2 = \bar{X}_S$  can be obtained. Since  $x_2 = 0$ ,  $x_3 = 0$ , and  $x_4 = 0$  are system invariants (ie. a system trajectory starting in an initial condition in this set, stays in this set for all future times), the system phase portrait in these sets are presented in separate figures for a better visibility.

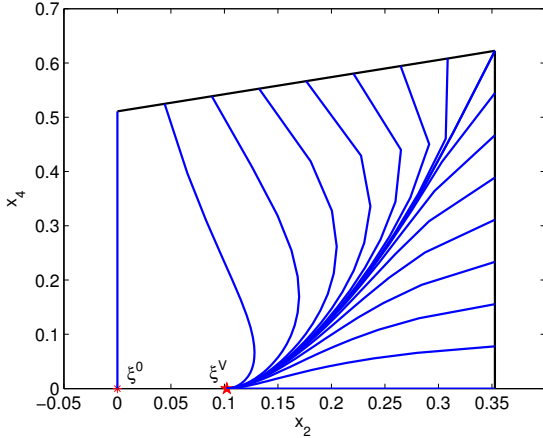


Fig. 4. The system phase portrait on the invariant set  $x_3 = 0$

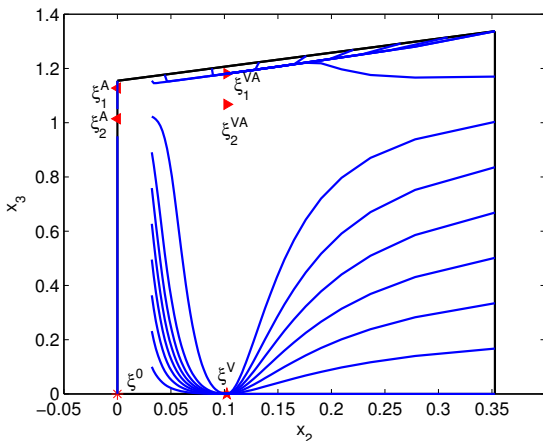


Fig. 5. The system phase portrait on the invariant set  $x_4 = 0$

Figs. 3- 5 respectively represent the system phase portrait on the invariants  $x_2 = 0$ ,  $x_3 = 0$  and  $x_4 = 0$ . The continuous black lines represent physical boundaries computed by respectively setting  $V = 0$ ,  $A = 0$  and  $H = 0$  in (21)-(23). Note that on  $x_2 = 0$ , a trajectory starting in an initial condition for which  $x_3 \neq 0$  converges either to  $\xi^0$  or  $\xi_1^{AH}$ , while a trajectory starting in an initial condition with  $x_3 = 0$  converges either to  $\xi^0$  or  $\xi_1^A$ . On the  $x_3 = 0$  invariant, all trajectories starting in initial conditions for which  $x_2 \neq 0$  converge to  $\xi^V$ , while a trajectory starting on the  $x_2 = 0$  axis stays on that axis and converges to  $\xi^0$ . On the  $x_4 = 0$  invariant, a trajectory starting on the  $x_2 = 0$  axis stays on this axis and converges either to  $\xi^0$  or  $\xi_1^A$ , while trajectories starting in initial conditions for which  $x_2 \neq 0$  either converge to  $\xi^V$  or  $\xi_1^{VA}$ . Fig. 6 shows the system phase portrait in the interior of the state space. Every trajectory starting in an initial

condition with  $x_2, x_3, x_4 \neq 0$  converges either to  $\xi^V$  or  $\xi_1^*$ , which is the equilibrium point characterized by the highest methane production among all the system equilibria for a certain dilution rate. However, the region of attraction of  $\xi_1^*$  is smaller than the one of  $\xi^V$ , which makes the system operation quite difficult.

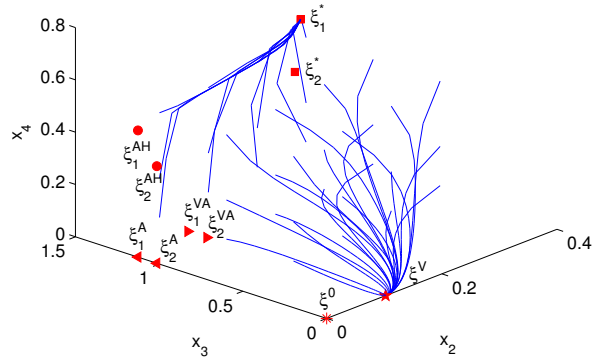


Fig. 6. The system phase portrait in the interior of the state space

## ACKNOWLEDGMENT

This paper presents research results of the Belgian Network DYSCO (Dynamical Systems, Control, and Optimization), funded by the Interuniversity Attraction Poles Programme, initiated by the Belgian State, Science Policy Office. The scientific responsibility rests with the authors.

## REFERENCES

- [1] D.J. Batstone, J. Keller, I. Angelidaki, S.V. Kalyuzhnyi, S.G. Pavlostathis, A. Rozzi, W.T.M. Sanders, H. Siegrist, and V.A. Vavilin, "Anaerobic Digestion Model No.1 (ADM1) (Scientific and Technical Report No. 13)", IWA Task Group for Mathematical Modelling of Anaerobic Digestion Processes, IWA Publishing, London, 2002.
- [2] G. Giovannini, M. Sbarciog, A. Donoso-Bravo, G. Ruiz-Filippi, and A. Vande Wouwer, "Derivation of a reduced-order dynamic model of anaerobic digestion using maximum likelihood principal component analysis", in "AD 14th IWA World Congress on Anaerobic Digestion", Vina del Mar, Chile, 2015.
- [3] D. Gaida, C. Wolf, C. Meyer, A. Stuhlsatz, J. Uppel, T. Bäck, M. Bongards, and S. McLoone, "State estimation for anaerobic digesters using the ADM1", *Water Sci. Technol.*, vol. 66, pp. 1088-1095, 2012.
- [4] A. Bornhöft, R. Hanke-Rauschenbach, and K. Sundmacher, "Steady-state analysis of the anaerobic digestion model No. 1 (ADM1)", *Nonlinear Dyn.*, vol.73, pp. 535-549, 2013.
- [5] M. Sbarciog, M. Loccufier, and E. Noldus, "Determination of appropriate operating strategies for anaerobic digestion systems", *Biochem. Eng. J.*, vol. 51, pp. 180-188, 2010.
- [6] B. Benyahia, T. Sari, B. Cherki, and J. Harmand, "Bifurcation and stability analysis of a two step model for monitoring anaerobic digestion processes", *J. Process Contr.*, vol. 22, pp. 1008-1019, 2012.
- [7] M. Weederdmann, G.S.K. Wolkowicz, and J. Sasara, "Optimal biogas production in a model for anaerobic digestion", *Nonlinear. Dyn.*, vol. 81, pp. 1097-1112, 2015.
- [8] K. Stamatelatos, L. Syrou, C. Kravaris, and G. Lyberatos, "An invariant manifold approach for CSTR model reduction in the presence of multi-step biochemical reaction schemes. Application to anaerobic digestion", *Chem. Eng. J.*, vol. 150, pp. 462-475, 2009.
- [9] A. Dhooge, W. Govaerts, and Y.A. Kuznetsov, "Matcont: A matlab package for numerical bifurcation analysis of odes", *ACM Trans. Math. Softw.*, vol. 29(2), pp. 141-164, 2003.